Cement & Concrete Composites 33 (2011) 368–379

Contents lists available at ScienceDirect

Cement & Concrete Composites

journal homepage: www.elsevier.com/locate/cemconcomp

Effect of autogenous deformation on the cracking risk of slag cement concretes

Aveline Darquennes [a,*], Stéphanie Staquet [a], Marie-Paule Delplancke-Ogletree [b], Bernard Espion [a]

[a] BATir Department, Université Libre de Bruxelles (ULB), F.D. Roosevelt Avenue 50 CP 194/2, B 1050 Brussels, Belgium
[b] Matières & Matériaux Department, Université Libre de Bruxelles (ULB), F.D. Roosevelt Avenue 50 CP 194/2, B 1050 Brussels, Belgium

ARTICLE INFO

Article history:
Received 15 July 2010
Received in revised form 9 December 2010
Accepted 11 December 2010
Available online 17 December 2010

Keywords:
Autogenous shrinkage
Cement matrix expansion
Relaxation
Time-zero
TSTM

ABSTRACT

Autogenous deformation under restrained conditions often leads to cracking and durability problems in concrete structures. It is therefore important to monitor accurately the early age development of autogenous deformation. However, its expression depends strongly on the measuring methods and on the choice of the time-zero. In order to determine the effect of slag on the evolution of autogenous deformation, a test rig was designed to monitor this deformation for three concretes with different slag content. The choice of different time-zero was also discussed based on different methods: setting evolution, time of peak expansion and evolution of deformation rate. Moreover, their restrained shrinkage was studied by means of a Temperature Stress Testing Machine (TSTM). Following these experiments, the slag cement concretes crack later than the Portland cement concrete despite the fact that they are characterized by a larger autogenous shrinkage. This behavior is mainly due to the expansion of their cement matrix at early age and their largest capacity to relax internal stresses.

1. Introduction

Slag cement concretes present many advantages in comparison with Portland cement concretes. Indeed, production of slag cements requires less energy and emits less carbon dioxide in the atmosphere [1]. Moreover, this kind of concrete is also characterized by a lower hydration heat, a lower permeability and a better resistance to sulphate attack [2,3]. Because of these various advantages, the use of slag cement concretes is spreading for all kinds of constructions and civil engineering structures (e.g. highways, bridges, tanks...).

However, some structures built with slag cement concretes have exhibited early age cracking due to restrained shrinkage [4]. This susceptibility to cracking can be related to the evolution of autogenous shrinkage. Indeed, several authors observed a larger autogenous shrinkage for slag cement concretes than for Portland cement concretes [5,6]. Nevertheless, slag effect on the evolution of autogenous deformation and on its amplitude is not always clearly defined in the literature. For example, slag content [7] and time when the deformation is initialized [8], called hereafter time-zero [9], can modify the above conclusion. To determine the actual effect of autogenous shrinkage on cracking risk of slag cement concretes, it is therefore necessary to study in-depth the evolution of this deformation.

Furthermore, the study of autogenous deformation under free conditions requires the use of equipment limiting the errors related to the measuring method. Many test rigs are proposed in the literature for monitoring the evolution of autogenous deformation at early age. Some of them may suffer from measurement artifacts related to thermal gradients in the sample [10], restraint related to the mould at early age [11], friction between the sample and the mould [12]. For such reasons a new shrinkage testing device was developed in the laboratory of the Civil Engineering department at the Université Libre de Bruxelles (ULB). Its design is based on an extensive literature review [13] and aims at limiting these errors as much as possible. The device enables measurements directly after casting. This last characteristic is important because autogenous shrinkage has to be measured at very early age (<24 h) in order to obtain its maximum potential.

Another interesting point is that the reported evolutions of autogenous deformation strongly depend on the definition of the time-zero [14]. A wrong choice of this reference time can lead to different interpretations of behavior for the same material. In this paper, several definitions of time-zero were studied to obtain realistic interpretations of slag cement concrete behavior.

Finally, the occurrence of cracks inside cementitious materials also depends on other factors such as evolution of material strength, rigidity, and capacity to relax tensile stress, as well as the degree of restraint of the concrete element. All these parameters were studied in a parallel experimental campaign conducted with a Temperature Stress Testing Machine (TSTM) [15] to determine the cracking susceptibility of slag cement concretes under sealed conditions.

* Corresponding author.
E-mail address: adarquen@ulb.ac.be (A. Darquennes).

0958-9465/$ - see front matter © 2011 Published by Elsevier Ltd.
doi:10.1016/j.cemconcomp.2010.12.003

Table 1
Cements characteristics.

Cements	CEM I 52.5 N	CEM III A 42.5 LA	CEM III B 42.5 HSR LA
Clinker content (%)	95	58	27
Slag content (%)	–	42	71
Limestone filler content (%)	–	–	2
Specific area (m^2/kg)	445	447	477
Density (kg/m^3)	3.09	3.01	2.93

Table 2
Concretes mixtures proportions.

Composition (kg/m^3)	CEM I	CEM III/A	CEM III/B
Cement	375		
Water	164.6	166.95	164.9
Total water	169	169	169
Superplasticizer	5.63	2.63	5.25
Sand 0/0.5	492	492	492
Sand 0.5/1	126	126	126
Sand 1/3	104	104	104
Limestone 2/6	311	311	311
Limestone 6/10	438	438	438
Limestone 10/14	415	415	415
Slump (mm)	80	80	130

2. Experimental program

2.1. Materials

Three cements were used in this experimental program: a Portland cement CEM I 52.5 N and two blended cements namely CEM III/A 42.5 LA and CEM III/B 42.5 HSR LA. The blended cements (CEM III/A 42.5 LA and CEM III/B 42.5 HSR LA) contained 42% and 71% of slag respectively. The clinker and the slag of the three cements had the same origin. Their specific area and density were similar (Table 1). The chemical composition of the studied slag and clinker, a parameter affecting significantly the reactivity and mechanical properties [16] of cementitious material, is given in [17].

The concretes associated with these three cements are hereafter indicated as CEM I, CEM III/A and CEM III/B respectively. The water–binder ratio (w/b) and the binder (clinker + slag) content of these concretes were kept constant and equal to 0.45 and 375 kg/m^3 respectively. Crushed aggregates with six different fractions were used. The concrete mixture proportions are given in Table 2.

2.2. Testing procedure

2.2.1. Mechanical properties

The mechanical properties of the concretes were measured at 1, 3, 7, 14 and 28 days on three cylindrical samples (Ø = 100 mm and h = 200 mm for the compressive strength and 350 mm for the static elastic modulus) kept at 20 °C and 90% R.H. In order to determine the evolution of the material stiffness before 1 day, the measurements were supplemented by monitoring the dynamic modulus. This parameter can be calculated from the evolution of the ultrasonic velocity measured on concrete samples stored at 20 °C (Eq. (1), [18]). In this last equation, the Poisson coefficient varies with the advancement of the hydration reaction. It can be estimated from Eq. (2) [19], where the degree of the hydration reaction is calculated from the evolution of the chemically bound water content measured by thermogravimetry [17]. Notice that the evolution of the ultrasonic velocity was also used to determine the initial and final setting times of the studied concretes [17].

$$E_d = V^2 \frac{\rho(1+\upsilon)(1-2\upsilon)}{(1-\upsilon)} \quad (1)$$

$$\upsilon(\alpha) = 0.18 \sin\left(\frac{\pi\alpha(t)}{2}\right) + 0.5\exp(-10\alpha(t)) \quad (2)$$

where E_d, V, υ, ρ and α are the dynamic elastic modulus (Pa), the ultrasonic velocity (m/s), the Poisson coefficient, the density (kg/m^3) and the hydration degree respectively.

2.2.2. Free autogenous deformation

Fig. 1 presents the testing equipment developed for monitoring free autogenous deformation directly after casting. Concrete was cast in a cylindrical Teflon mould (Ø = 96 mm and h = 210 mm) which allows minimizing the friction between the sample and the mould walls. Since the thermal expansion coefficient of Teflon (80×10^{-6}/°C) is much larger than that of concrete (10×10^{-6}/°C), the mould did not counteract concrete volume variations related to the temperature increase. A Teflon mould was also used in other research studies [10,20]. Nevertheless, our experimental device differs by its deformation measurement set-up and the use of a thermal regulation system directly in contact with the mould. Indeed, the linear contraction/expansion of the samples was measured by means of two displacement transducers (Solartron LE12) in contact with steel plates anchored at the ends of the samples. The use of two transducers allows measuring the relative displacement between the top and the bottom of the sample. The measuring range of these transducers is 12 mm with an accuracy of 0.4 μm. They were mounted on a rigid frame with vertical posts in invar. This material is characterized by a low thermal dilation coefficient (1.6×10^{-6}/°C). In that way the effects of ambient temperature variations on the measurements are minimized. Unlike the two other equipments [10,20], the specimens were immersed vertically in a temperature-controlled bath to limit thermal deformations. Thanks to this thermal regulation system, thermal gradients related to the sample sizes and the hydration reaction were inferior to 0.3 °C and 2 °C respectively during an isothermal test at 20 °C (for the Portland cement concrete). A plastic foil was put between the mould and the samples to insure water tightness. Displacement measurements in isothermal conditions were supplemented by temperature measurements (bath water, ambient air, concrete) to investigate the influence of the temperature on the measured parameters. This experimental device was validated

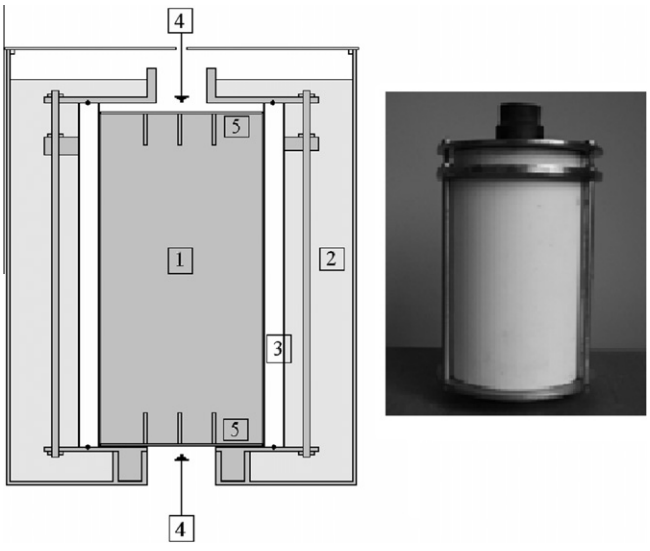

Fig. 1. The autogenous deformation equipment and its mould (1. concrete sample, 2. vessel, 3. Teflon cylindrical mould, 4. displacement transducers position, 5. steel plates with anchorages).

comparing shrinkage measurements on Portland cement concrete obtained with the BTJADE equipment (LCPC, Paris) developed by Boulay [21].

For each concrete, several specimens from different batches were tested at 20 °C [13]. The evolution of their autogeneous deformation was expressed as function of the equivalent age. This analysis allows removing the influence of temperature on the maturity of concrete samples. The validity of the maturity approach applied to autogenous shrinkage measurements is always a controversial issue. Indeed, some authors [22,23] suggest that this approach should not be applied to predict autogenous deformation. Others [24–26] have a different, though often nuanced, position. Turcry et al. [25] assume that the maturity approach is valid for temperature values varying from 10 °C to 40 °C. Kamen et al. [26] limit the temperature interval between 20 °C and 30 °C. In this study, the temperature variation was around 20 °C. Thanks to this low temperature variation, this approach can thereafter be applied.

These experimental results were also compared with results obtained with the TSTM device. In this last case, free conditions were obtained by cancelling the load applied to the sample once the stress inside concrete reached the value of 0.01 MPa. This equipment is described in the following section.

2.2.3. Restrained autogenous deformation

The restrained autogenous deformation was monitored using the TSTM equipment. In the framework of this study, the frame of TSTM was equipped with a mould and thermal regulation and displacement measurement systems. The TSTM consists of an electromechanical testing setup, where one end of the specimen is restrained by a steel head and the displacement of the other is controlled by a motor moving the other steel head (Fig. 2). The dog-bone sample was characterized by a cross-section equal to $100 \times 100\ mm^2$ in its center and $100 \times 150\ mm^2$ at its extremities. The straight part (center of the specimen) was 1 m long. The mould of the sample was made of aluminium and its inner surface was covered with a Teflon sheet to minimize friction. Before casting the concrete, a thin plastic film was installed in the framework to prevent water evaporation. Isothermal conditions were obtained by means of a thermal regulation system consisting of several zinc box beams placed in contact with the mould. Thanks to this system, the thermal gradient related to the hydration process was limited to a value inferior to 1 °C for a Portland cement concrete. Furthermore, thermal conditions tended to stabilize after 100 min. These values are close to the ones obtained with other TSTM devices [15,26,27]. Displacements were measured by means of two transducers (Solarton LE12) placed on the straight part of the sample and separated by 750 mm to limit the effects of boundary conditions. They were mounted on a rigid frame fixed to the TSTM. These sensors were in contact with an invar rod screwed on a threaded rod anchored in the sample directly after casting. The invar rods were kept in their initial position thanks to a brass ring until the beginning of the tests. The evolution of the temperature was also monitored using a thermocouple placed in the concrete specimen.

Restrained shrinkage was measured as follows (Fig. 3): the sample placed in the TSTM was initially restrained by the stiffness of the frame with the motor being turned off until stresses inside concrete reached a threshold value of 0.01 MPa. At that moment, the displacement transducer readings were zeroed and the concrete sample could deform freely until the recorded deformation in the central part of the specimen reached a threshold equal to 6.7 μm/m ($\Delta\varepsilon_{limit}$ in Fig. 3). This moment coincides with the end of the first cycle. Then, the load was adjusted to pull the specimen back to its initial length. The applied load at the end of the adjustment process was kept constant during the following cycle until the deformation in the sample reached again the previous threshold value. This procedure was applied many times till cracking of the specimen and it is similar to the one used by Charron et al. [15]. It allows avoiding early cracking of the specimen. During the test, four parameters were continuously monitored: the load applied on the sample, its deformation, its temperature and the displacement of the moving head.

2.2.4. Microstructure evolution

The previous macroscopic analysis on the autogenous deformation of slag cement concretes was completed by a microscopic study to determine the slag effect on the nature and evolution of the hydration products. The evolution of portlandite, ettringite and chemically bound water content were monitored by means of different techniques: differential thermal analysis (DTA), thermogravimetry (TGA), differential scanning calorimetry (DSC) and scanning electron microscopy (SEM). They were applied on mortar samples extracted from fresh concrete kept at 20 °C and 90% R.H. Their hydration reaction was stopped at different ages ($\leqslant$1, 2, 3, 7 and 28 days) using two solvents (ethanol and ether). Capillary porosity and pore size distribution of the samples were also quantified by means of a mercury porosimeter able to detect pores with diameters ranging from 360 μm to 0.003 μm. In the following, capillary porosity is considered within the interval characterized by pore diameter between 5 μm and 0.01 μm corresponding to the pore space between the binder grains [28]. Nevertheless, one has to keep in mind that such measures only quantify pores accessible to mercury and thus can lead to a wrong estimation of the pore size distribution of the cementitious material [29].

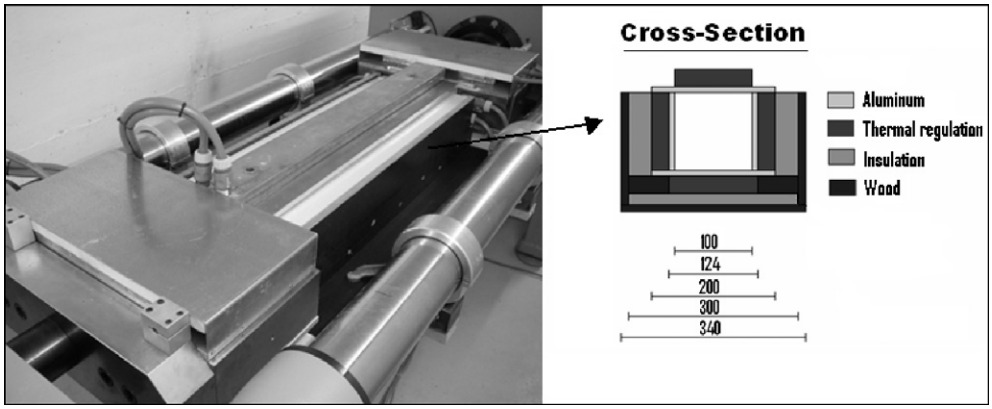

Fig. 2. The TSTM equipment with dog-bone sample and the cross-section in the straight part of its mould with a thermal regulation system (measurements in mm).

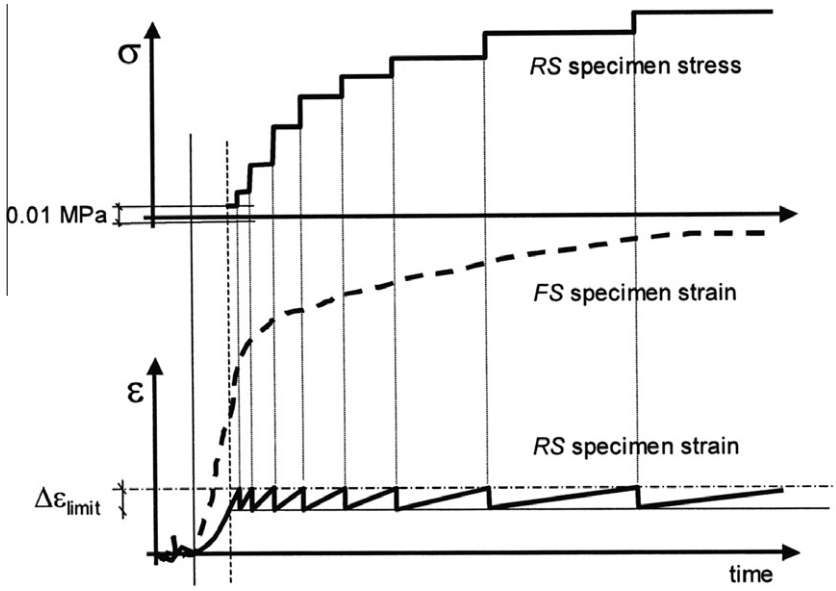

Fig. 3. Procedure of restrained shrinkage test from [15].

Table 3
Evolution of average compressive strength and static elastic modulus.

Age (days)	CEM I		CEM III/A		CEM III/B	
	fc (MPa)	*E* (GPa)	fc (MPa)	*E* (GPa)	fc (MPa)	*E* (GPa)
1	26	32	14	31	3	22
3	41	38	30	36	26	36
7	49	40	47	41	45	41
28	54	43	61	45	56	45

3. Experimental results and discussion

3.1. Mechanical properties

At early age, the slag cement concretes are characterized by a lower strength than the Portland cement concrete (Table 3). This behavior is due to their low C_3S content [30] and to the evolution of their hydration reaction consisting of two subreactions: a clinker and a slag reaction [3]. Indeed, hydration of slag cement concretes depends on the breakdown and the dissolution of the glassy slag structure caused by hydroxyl ions released during hydration of the clinker and alkali content in cement [31]. Moreover, the portlandite resulting from the clinker reaction is needed by slag reaction to product additional C–S–H. This is why the evolution of strength at early age is delayed for slag cement concretes. At 7 days, their strength value is close to that of CEM I.

For CEM III/B, evolution of static elastic modulus is close to the evolution of its compressive strength: a low value at early age and a fast increase during the first days. The static elastic moduli of CEM I and CEM III/A are similar from 1 day. After 3 days, the values of static moduli of all the studied concretes are almost the same and evolve slowly.

3.2. Free autogenous deformation

3.2.1. The time-zero

Evolution of the autogenous deformations has to be expressed from the time-zero defined as the time when stresses appear [9]. Several ways based on the initial or final setting time [32,33], time of peak expansion [34], deformation rate [35] and self-induced stresses evolution [36] are proposed in the literature to determine time-zero. The first three methods are discussed hereafter.

According to the first method, autogenous deformation is often expressed from the initial setting time. In our case, this time was measured and found equal to 5.5 h, 5 h and 7 h for CEM I, CEM III/A and CEM III/B respectively. Thanks to the expansion of their cement matrix at early age, autogenous shrinkage of the slag cement concretes expressed in that way presents a lower value than autogeneous shrinkage of the Portland cement concrete at 28 days (Fig. 4). This definition of time-zero is generally chosen because the material stiffness, a parameter providing an indication about the ability of the material to develop internal stresses, changes rapidly during the setting.

However, according to our experimental results (Fig. 5), the values of the moduli of the studied concretes are negligible at the initial setting time and then they increase slowly during the setting. At the final setting time located at 9 h, 8.8 h and 10.5 h for CEM I, CEM III/A and CEM III/B respectively, moduli are still low. They are equal to 11 GPa, 5 GPa and 2 GPa respectively. In other words, significant stresses do not develop during the setting. Following this observation, it seems that a reference time equal to the final setting is more appropriate. This choice is in agreement with the results of Sant et al. [32]. Autogenous deformation of the slag cement concretes expressed from this time-zero is still characterized by an expansion of their cement matrix and the value of their shrinkage at 28 days is always inferior to the shrinkage value of the Portland cement concrete.

According to Cusson [34], the cracking risk of concretes characterized by an expansion of the cement matrix at early age is underestimated if the extent of free shrinkage is expressed from a time-zero based on the setting. The reason is that not all of the strain will produce tensile stresses under restrained conditions. A conservative estimate of the deformation that may produce cracking in concrete structures for this kind of concrete may be obtained if autogeneous deformation is expressed from the peak of expansion of the cement matrix [34]. When applying this approach, the slag cement concretes are characterized by a larger value of shrinkage at 28 days than the Portland cement concrete (with deformation initialized from the final setting time) (Fig. 6). It also appears that shrinkage evolution rate is the largest.

These various approaches require monitoring the setting for the Portland cement concrete, a material without expansion of its

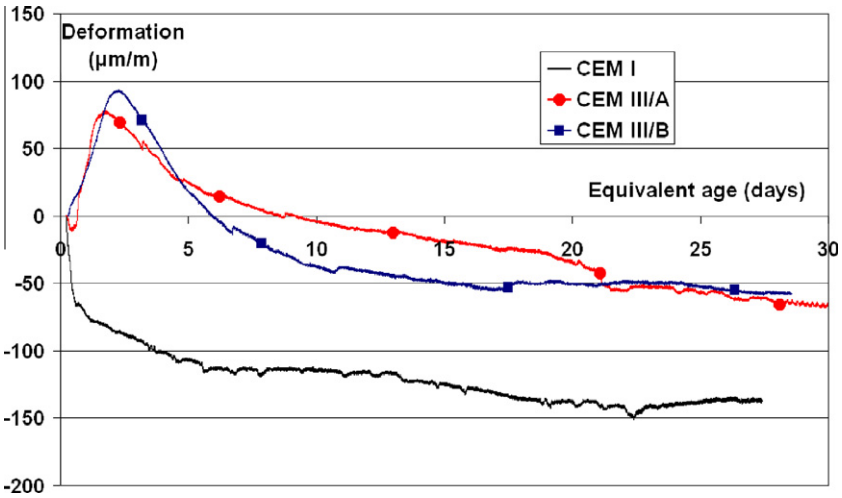

Fig. 4. Autogenous deformations expressed from the initial setting: 5.5 h, 5 h and 7 h for CEM I, CEM III/A and CEM III/B respectively.

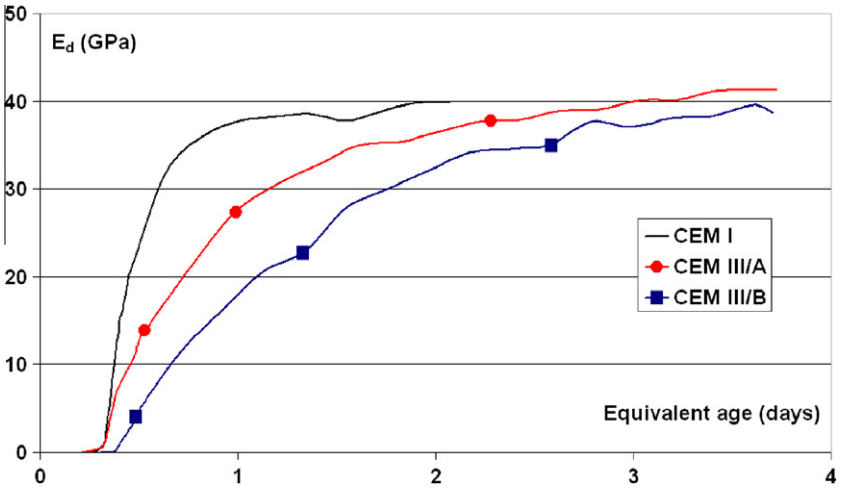

Fig. 5. Evolution of the dynamic elastic modulus.

cement matrix at early age. However, evolutions of setting and autogenous deformation are not determined on the same specimen. Therefore, the hydration reaction advancement of these concrete specimens could be different due to errors related to experimental conditions (ambient temperature, dimensions of the sample, batches, etc.). In order to limit the errors, it would be better if one could determine time-zero and deformation evolution on the same sample. A way to do this is to determine time-zero thanks to the evolution of the shrinkage rate.

Following this third method, time-zero is defined as the moment characterized by the second maximal value of the deformation rate (Fig. 7). For the slag cement concretes, this time is located between the final setting time and the end of the expansion period of the cement matrix (Fig. 8). It is equal to 20.5 h, 30 h and 55 h for CEM I, CEM III/A and CEM III/B respectively. This definition of the time-zero can be viewed as the time when significant stresses develop inside the concrete samples. Indeed, the rate of deformation decreases after this moment due to the increasing stiffness of the material. This hypothesis was confirmed thanks to restrained shrinkage tests realized with the TSTM. These experiments showed that this moment is also close to the moment when internal stresses equal to 0.01 MPa appear inside the sample [13]. A similar reference time was also chosen by other authors [35,36].

In comparison with the previous method based on the time of expansion peak, this approach underestimates slightly the final shrinkage value of CEM I and CEM III/A. But at 28 days, the slag cement concretes are again characterized by a larger autogenous shrinkage than CEM I. Furthermore, the autogenous deformation curves of concretes from same or different batches expressed from this time-zero (Fig. 7) show a small difference (<20 µm/m). This result can be compared with the experimental campaign presented in [37]. In this study, the autogenous deformation curves expressed from 3 days for the same mix from different batches show a difference equal approximately to 30 µm/m. Using the evolution of the shrinkage rate seems thus to be the most reliable method to define the time-zero in the framework of this work about the cracking risk of the slag cement concretes.

3.2.2. Expansion of the cement matrix

As it has been already mentioned, autogenous deformation of the slag cement concretes is characterized by expansion of the cement matrix at early age (Fig. 4). This was also observed by other authors [8,38]. This phenomenon is significant because it delays the occurrence of the autogenous shrinkage.

In the literature, cement matrix expansion at early age under isothermal conditions for different types of cementitious materials

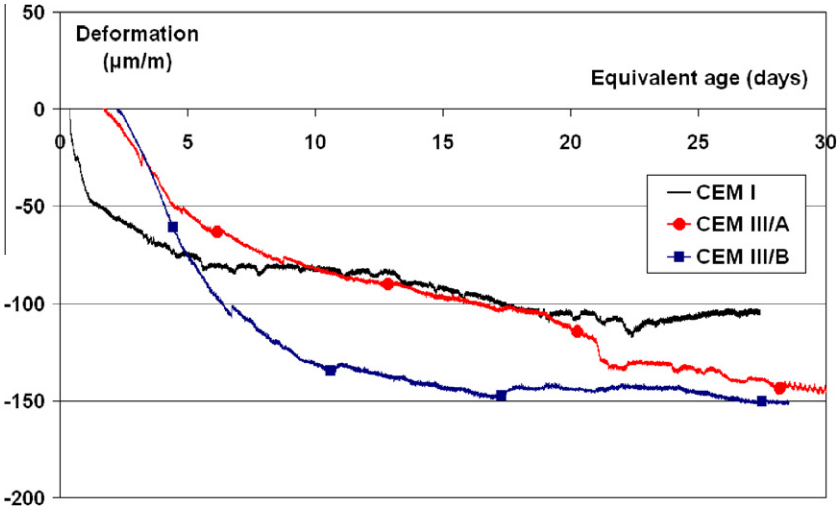

Fig. 6. Autogenous deformations expressed from the final setting for CEM I (9 h) et from the peak of expansion of the cement matrix for CEM III/A (1.76 days) and CEM III/B (2.26 days).

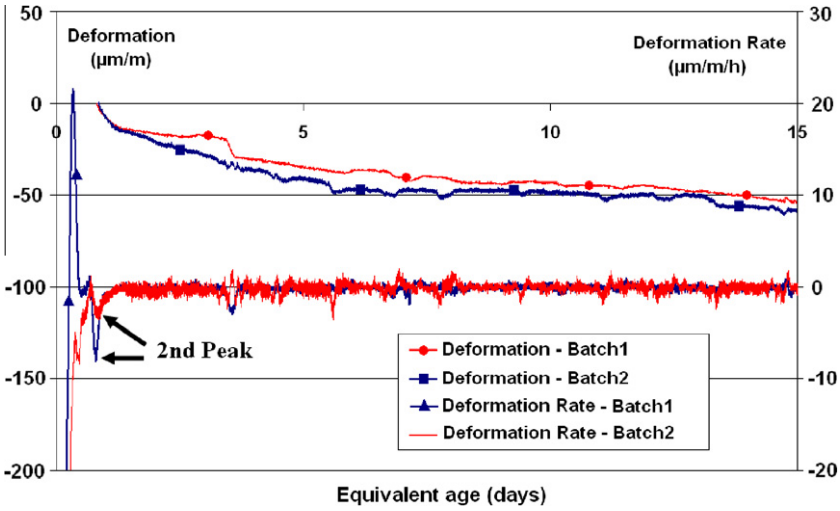

Fig. 7. Evolution of the deformation rate and the autogenous deformations expressed from the second maximal value of the deformation rate of the CEM I mix from two different batches.

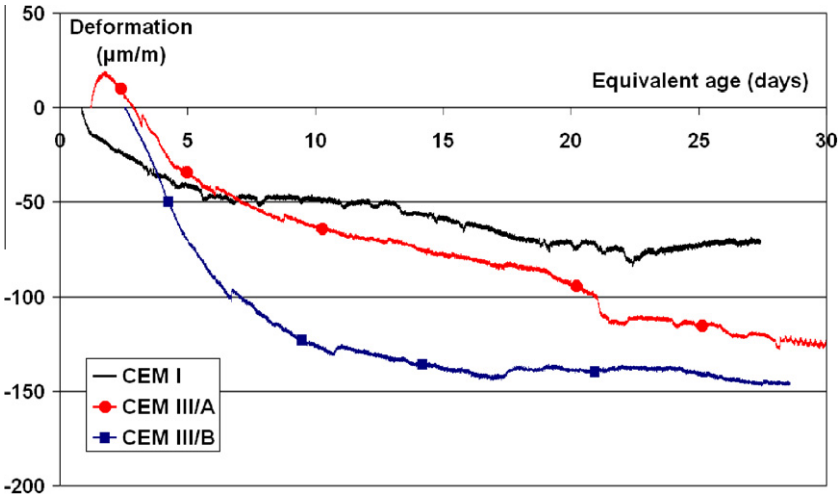

Fig. 8. Evolution of the autogenous deformations expressed from a moment characterized by the second maximal value of deformation rate (20.5 h, 30 h and 55 h for CEM I, CEM III/A and CEM III/B respectively).

is often related to the occurrence and growth of hydration products ($Ca(OH)_2$, Afm, Aft) [39], an internal C–S–H growth [40], a reabsorption of the bleeding water [23] or a measuring artifact (e.g. thermal gradients inside the concrete sample). In this experimental campaign, cement matrix expansion is not due to a temperature variation linked to the hydration reaction. Indeed, thermal dilatation is very limited (less than 12 μm/m) thanks to the good thermal regulation system around the samples (Fig. 1). Moreover, cement matrix expansion was also measured by means of the TSTM measuring the free autogenous deformation at early age [13]. It seems thus that cement matrix expansion of the slag cement concretes is a material behavior.

To better understand this observation, the evolutions of autogenous deformation, elastic modulus and portlandite content are compared in Figs. 9 and 10. During expansion, the elastic moduli of the mixtures increase rapidly (E = 36 GPa and 33 GPa at the expansion peak for CEM III/A and CEM III/B respectively) as well as the portlandite content for CEM III/A. This last observation was also confirmed by SEM analysis (Fig. 11, left) showing clearly portlandite crystals at 2 days. On the contrary, the portlandite content for CEM III/B remains (almost) constant. The reason is that it is used by slag hydration to produce additional C–S–H. Indeed, C–S–H is apparent on SEM pictures from 3 days (Fig. 12). During the first 2 days, SEM analysis showed that the main hydration product is ettringite (Fig. 11, right).

In order to monitor the development of ettringite, the consumption of the setting regulator by the mineral phases of clinker C_3A and C_4AF to produce ettringite was measured with DSC. More specifically we looked at the evolution of the endothermic peak located between 120 and 160 °C (Figs. 13 and 14). This peak vanishes after 1 and 3 days for CEM III/A and CEM III/B respectively. These previous observations confirm that the expansion phase of slag cement concretes is characterized by a fast ettringite development.

It appears thus that the expansion of slag cement matrix is related to the formation of hydration products which apply crystalline pressures on the pore surfaces against which the growing rigidity of the cement matrix cannot compete.

3.2.3. Slag effect

Considering the evolution of autogenous deformations initialized from a time-zero equal to the moment characterized by the second maximal value of the deformation rate, it appears that the deformations of both slag cement concretes are larger than that

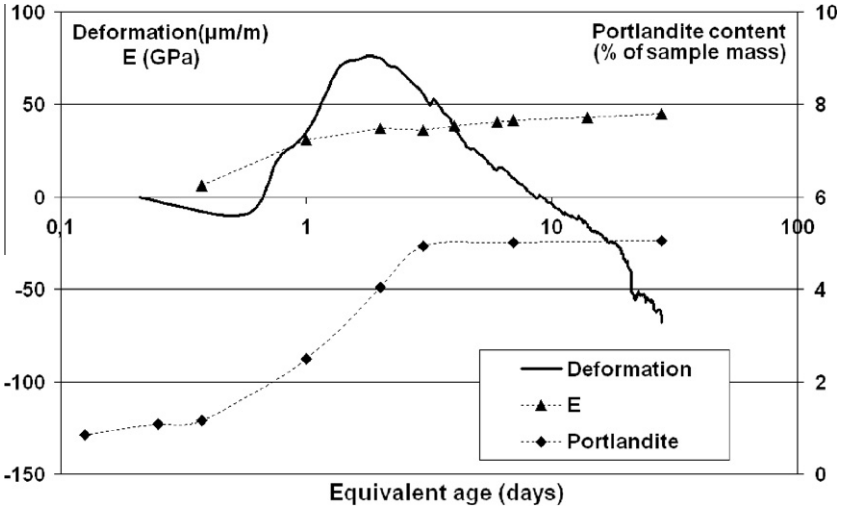

Fig. 9. Evolutions of the portlandite content, static elastic modulus and autogenous deformation initialized from the initial setting for CEM III/A.

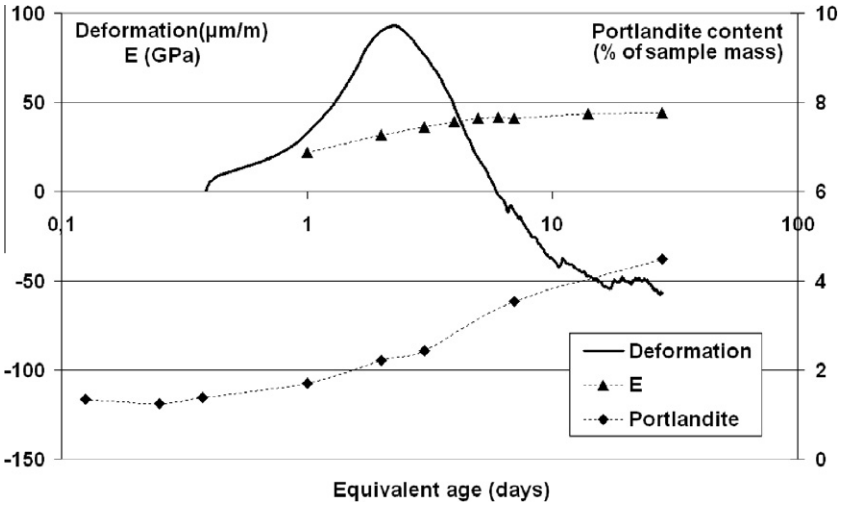

Fig. 10. Evolutions of the portlandite content, static elastic modulus and autogenous deformation initialized from the initial setting for CEM III/B.

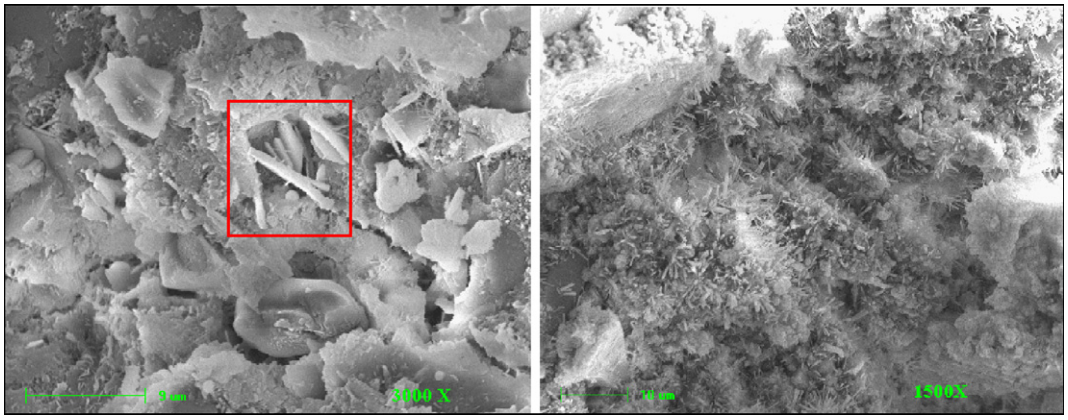

Fig. 11. Hydration products of CEM III/A (left – square: portlandite) and CEM III/B (right) at 2 days.

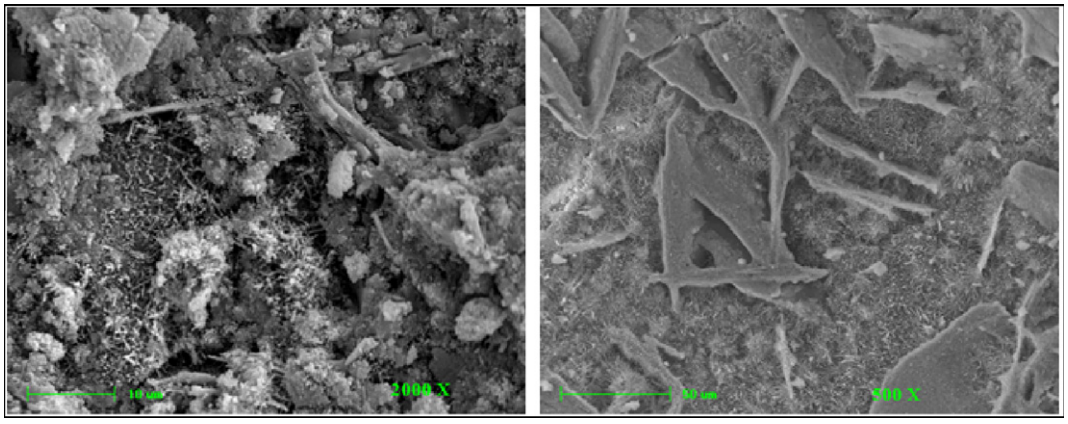

Fig. 12. Hydration products of CEM III/B at 3 days: ettringite (left) and C–S–H (right).

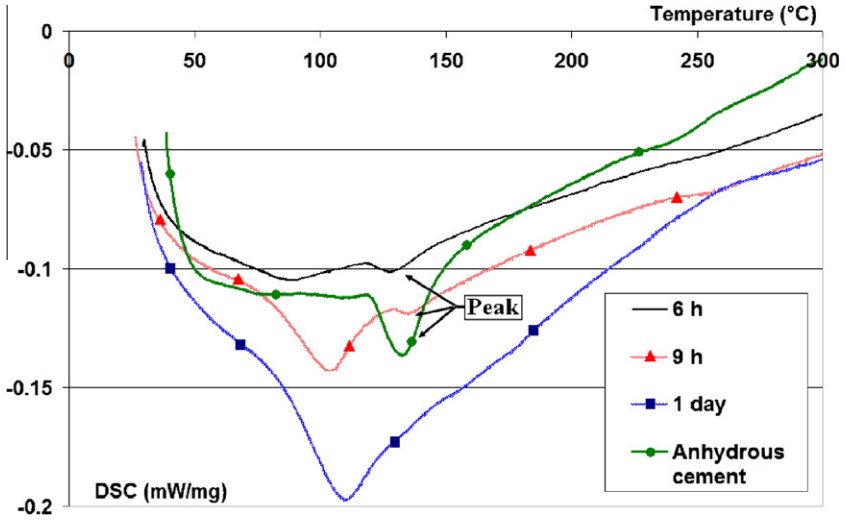

Fig. 13. Thermal analysis of CEM III/A by DSC.

of CEM I after 7 days (Fig. 8). This behavior was confirmed by the experimental tests realized with the TSTM under free conditions (Fig. 15). More specifically, comparison of the autogenous shrinkage curves obtained by the two experimental devices (Figs. 8 and 15) shows that deformations of the slag cement concretes at 6 days measured on the dog-bone sample are slightly larger than the ones measured on the cylindrical sample. This difference of behavior is related to the amplitude of their expansion phase which is lower for the measurements realized with the TSTM. This lower amplitude is due to the stiff frame of the TSTM that restricts cement matrix expansion.

Autogenous shrinkage increases thus faster for the slag cement concretes than for the Portland cement concrete with the advancement of the hydration reaction. Moreover, the CEM III/B mix is

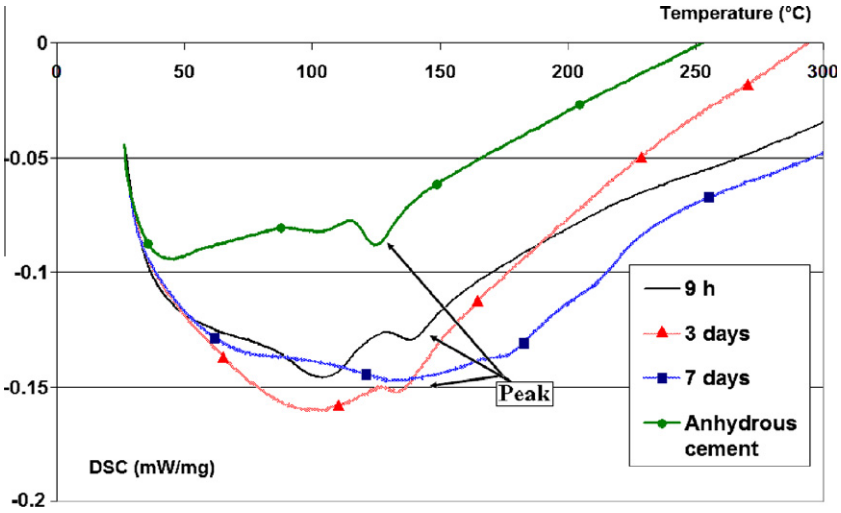

Fig. 14. Thermal analysis of CEM III/B by DSC.

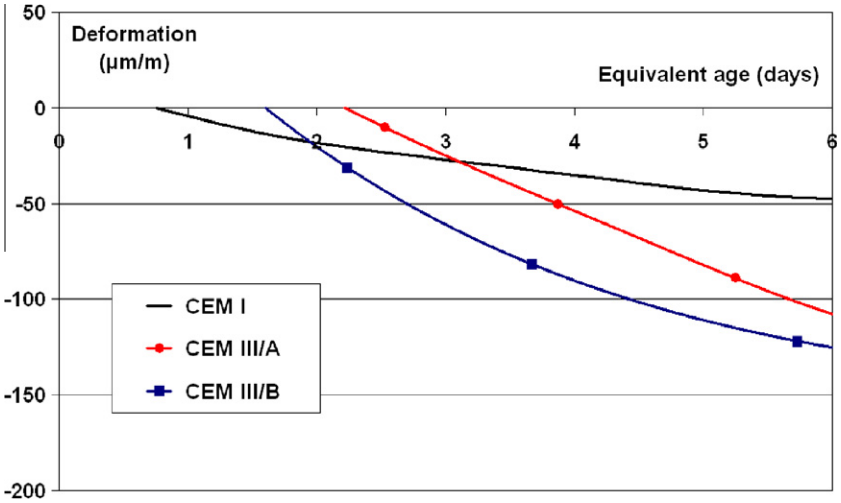

Fig. 15. Evolution of the autogenous deformations measured with the TSTM and expressed from a time-zero equal to the moment characterized by the second maximal value of the deformation rate measured with the autogenous deformation device.

characterized by the highest value of shrinkage at 28 days. The difference of behavior between CEM III/A and CEM III/B is only related to the slag effect on the hydration kinetics. Indeed, their deformation rate is similar beyond the expansion phase, when deformations are expressed as function of the hydration degree. However, this last point is not sufficient to explain the difference of behavior between the slag and Portland cement concretes.

The major mechanism at the origin of self-desiccation is the variation of capillary depression. According to the Laplace and Kelvin laws, the intensity of capillary depression is inversely proportional to the pore radius. Thus, monitoring porosity evolution is a first approach to understand the difference of behavior between the slag and Portland cement concretes. At early age, capillary porosity is larger for CEM III/B and CEM III/A than for CEM I (Table 4). It decreases rapidly for the slag cement concretes. At 7 days, all concretes present the same percentage of capillary porosity. The curves of cumulative porosity show that pore size is larger for CEM III/B than for CEM I and CEM III/A at 2 days (Fig. 16). With the advancement of the hydration reaction, this difference of behavior vanishes. At 7 days, pore size distribution is almost the same for all studied concretes. This observation could be explained by the production of additional C–S–H by the slag hydration filling

Table 4
Evolution of the capillary porosity (%).

	2 days	3 days	7 days	28 days
CEM I	15	15	13	10
CEM III/A	17	15	13	12
CEM III/B	19	17	13	13

the porosity developed at early age. The quantity of the finest pore size (diameter less than 15 nm) is slightly larger for CEM III/B. However, this last result has to be considered cautiously because the mercury porosimetry tends to underestimate the content of large pores and overestimate the content of small pores [29].

One possible explanation for the difference of shrinkage behavior between the slag and Portland cement concretes could be related to their finer and larger porosity leading to a larger capillary depression. This observation is in agreement with Lura's internal relative humidity results [38]. In his study, slag cement pastes were characterized by a lower internal relative humidity than Portland cement pastes. According to the Kelvin equation, pores are finer for slag cement pastes than for Portland cement pastes.

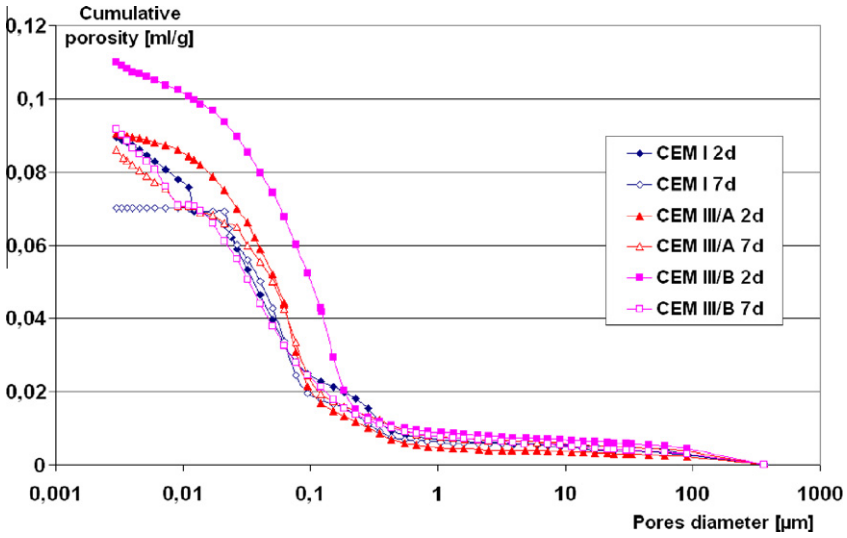

Fig. 16. Cumulative porosity at 2 and 7 days.

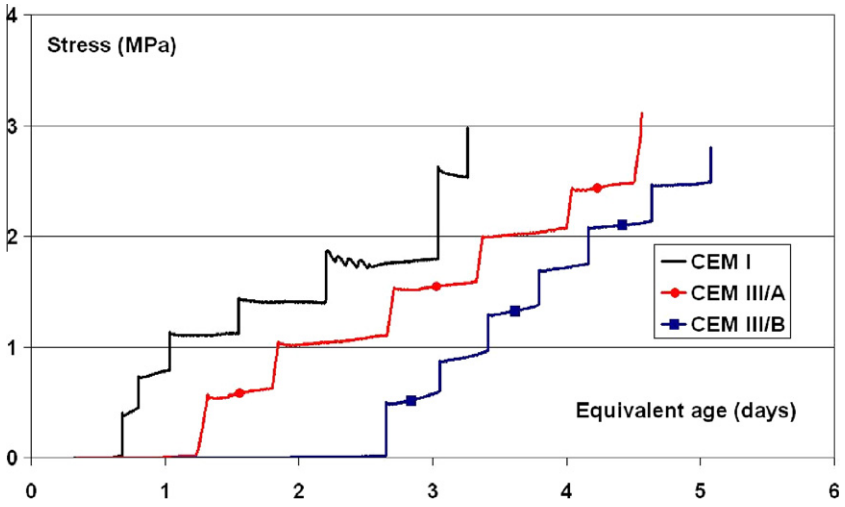

Fig. 17. Stress evolution at 20 °C under a complete degree of restriction.

3.3. Restrained autogenous deformation

Looking at the experimental results on the elastic modulus, strength and autogenous shrinkage, the slag cement concretes, especially CEM III/B, seem to be more prone to crack under restraint conditions than the Portland cement concrete. However, cracking risk also depends on other factors, such as the degree of restriction and the material capacity to relax tensile stresses.

These factors were taken into account in the retrained shrinkage tests realized with the TSTM equipment. They showed that autogenous shrinkage induced stresses develop faster for CEM I than for the slag cement concretes (Fig. 17). This difference is partially due to the cement matrix expansion of the slag cement concretes which delays the occurrence of the tensile stresses threshold (0.01 MPa). This threshold was used to start the tests (§2.2.3). It was reached at 15.4 h, 25.7 h and 55.7 h for CEM I, CEM III/A and CEM III/B respectively. Because of the fast increase in internal tensile stresses, CEM I cracks first at 3.3 days for a stress equal to about 3 MPa. Cracking appears later for CEM III/A and CEM III/B at 4.6 and 5.1 days respectively for a value of stress close to 3 MPa.

The theoretical stress value developed inside an elastic material can be calculated using the tests of free and restrained autogenous deformations (Eq. (3)). The difference between the evolution of the theoretical and measured stresses provides an estimation of the relaxation capacity of the studied concretes (Fig. 18). It appears that the slag cement concretes are characterized by a larger capacity to relax tensile stresses than the Portland cement concrete. Indeed at 3 days, relaxation is larger for the slag cement concretes than for the Portland cement concrete. One has to keep in mind that this estimation is based on several hypotheses: the restrained sample is not spoiling, the development of its modulus is similar to that of the free sample and the theory of superposition of deformations and stresses is valid. However, the largest capacity to relax stresses of the slag cement concretes was also confirmed by sealed tensile and compressive creep tests presented in [13].

$$\sigma_{el}(t_i) = \sigma_{el}(t_{i-1}) + \frac{E(t_i) + E(t_{i-1})}{2}(\varepsilon(t_i) - \varepsilon(t_{i-1})) \quad (3)$$

where $\sigma_{el}(t_i)$ is the theoretical stress at time t_i developed inside an elastic material (MPa), $E(t_i)$ is the tangent elastic modulus at time t_i calculated from deformations and stresses under restrained conditions and $\varepsilon(t_i)$ is the deformation under free conditions at time t_i for a time t_0 deduced from the shrinkage rate.

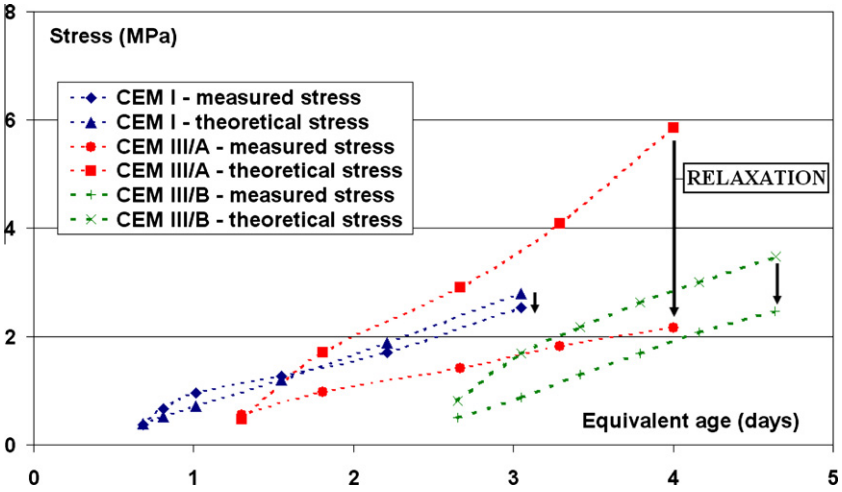

Fig. 18. Evolution of the theoretical and measured stresses at 20 °C.

Nevertheless, the reason of cracking delay of the slag cement concretes is not only related to their larger capacity to relax internal stresses. Indeed, relaxation capacity grows up later for all studied concretes (Fig. 18). Therefore, cracking delay of the slag cement concretes is also related to the expansion of their cement matrix at early age.

4. Conclusions

In this paper, an experimental program was presented in order to study the effect of autogeneous deformation on the cracking risk of slag cement concretes. The main achievements and observations are summarized hereafter:

- In order to determine the slag effect on the evolution of free autogenous deformation we have developed a specialized testing equipment minimizing measurement artifacts and monitoring deformation directly after concrete casting. The experimental campaign showed that the evolution of autogenous deformation strongly depends on the definition of time-zero, especially for the slag cement concretes characterized by an expansion of their cement matrix. In this work, three definitions of time-zero were considered: the initial or final setting time, the time of peak expansion and the time characterized by a maximal value of the deformation rate. This last definition was chosen as time-zero. It should be seen as the time from which significant stresses develop inside the concrete specimen. This assumption was confirmed by TSTM tests where tensile stresses were detected. This choice allows determining autogenous deformation and time-zero on the same sample, helping thus to avoid experimental errors. It also enables to take into account a large part of the deformation producing tensile stresses into the material under restrained conditions.
- The expansion of the cement matrix of the slag cement concretes is related to the fast formation of hydration products (C–S–H, ettringite, portlandite) at early age. They apply crystalline pressures on the pores surface against which the growing rigidity of the cement matrix cannot compete. Expansion has significant role because it delays the occurrence of autogenous shrinkage.
- The slag cement concretes are characterized by a larger value of shrinkage at 28 days than the Portland cement concrete. Their shrinkage evolution rate is also faster. This difference is principally due to their porosity. From the evolution of their elastic modulus, compressive strength and autogenous shrinkage, one could conclude that the slag cement concretes, especially CEM III/B, are more prone to crack under restrained conditions than the Portland cement concrete.
- Experiments realized with the TSTM equipment showed that the cracking susceptibility of the slag cement concretes is delayed in comparison with the Portland cement concrete. This behavior is due to their slower hydration kinetics, their larger capacity to relax tensile stresses and the expansion of their cement matrix at early age.

Based on these experimental results, it seems that the susceptibility to cracking of slag cement concrete under drying conditions is not directly related to the evolution of autogenous shrinkage. Therefore, autogenous deformation is not the major factor controlling this behavior.

Acknowledgements

This research is partially financed by grants funded by the Belgian National Foundation for Scientific Research (FRFC), which is gratefully acknowledged. The authors would also like to thank the research and testing departments of the Belgian Centre for scientific and technical research of the cement industry (CRICC-OCCN) for their contribution to this study.

References

[1] De Larrard F. Quelques questions soulevées par analyses du cycle de vie des infrastructures routières. Bull Lab Ponts Chaussées 2009;276:1–8.
[2] Bijen J. Blast furnace slag cement for durable marine structures. CIP Royal Library Den Haag, Stichting Betonprisma, 's-Hertogenbosch, The Netherlands; 1998. 62 pp.
[3] Roy DM, Idorn GM. Hydration, structure, and properties of blast furnace slag cements, mortars, and concrete. ACI J 1983(November–December):444–57.
[4] Darquennes A, Staquet S, Espion B. Cracking sensitivity of slag cement concrete. In: Marchand J, Bissonnette B, Gagné R, Jolin M, Paradis, F, editors. 2nd International symposium on advances in concrete through science and engineering, 11–13 September, Québec City, Canada; 2006. p. 311.
[5] Chern JC, Chan YW. Deformations of concrete made with Blast-furnace slag cement and ordinary Portland cement. ACI Mater J 1989;86:372–82.
[6] Tazawa E, Miyazawa S, Kasai T. Chemical shrinkage and autogenous shrinkage of hydrating cement paste. Cem Concr Res 1995;25:288–92.
[7] Lim SN, Wee TH. Autogenous shrinkage of ground-granulated blast-furnace slag concrete. ACI Mater J 2000;97:587–93.
[8] Aly T, Sanjayan JG. Shrinkage cracking properties of slag concretes with one-day curing. Mag Concr Res 2008;60:41–8.
[9] Bentur A. Early-age shrinkage and cracking in cementitious systems. Concr Sci Eng 2001;3:3–12.
[10] Brooks JJ, Megat Johari MA, Mazloom M. Autogenous shrinkage of high strength concrete from very early age. In: The 9th BCA annual conference on

higher education and the concrete industry, Cardiff University; 1999. p. 219–29.
[11] Lee KM, Lee HK, Lee SH, Kim GY. Autogenous shrinkage of concrete containing granulated blast-furnace slag. Cem Concr Res 2006;36:1279–85.
[12] Barcelo L, Boivin S, Rigaud S, Acker P, Clavaud B, Boulay C. Linear vs. volumetric autogenous shrinkage measurement: material behaviour or experimental artefact?, self-desiccation and its importance in concrete technology. In: Persson B, Fagerlund G, editors. Proceedings of the second international research seminar, 18 June, Lund; 1999. p. 109–25.
[13] Darquennes A. Comportement au jeune âge de bétons formulés à base de ciments au laitier de haut-fourneau en condition de déformations libre et restreinte. PhD thesis. Belgium: Université Libre de Bruxelles; 2009. 334p [in French].
[14] Weiss J. Experimental determination of the time zero t_0. In: Bentur A, editor. Early age cracking in cementitious systems, report of RILEM technical committee TC 181-EAS, report 25; 2003. p. 220–33.
[15] Charron JP, Bissonnette B, Marchand J, Pigeon M. Test device for studying the early-age stresses and strains in concrete. In: Jensen OM, Bentz DP, Lura P, editors. ACI SP-220; 2004. p. 113–24.
[16] Bougara A, Lynsdale C, Milestone NB. Reactivity and performance of blast-furnace slags of differing origin. Cem Concr Compos 2010;32:319–24.
[17] Darquennes A, Staquet S, Kamen A, Delplancke-Ogletree M-P, Espion B. Early age properties development of concrete with different slag contents. In: ACI SP-259, transition from fluid to solid: re-examining the behavior of concrete at early ages, 15–19 March, San Antonio, Texas, USA; 2009. p. 43–66.
[18] ASTM C597, standard test method for pulse velocity through concrete; 1997.
[19] De Schutter G, Taerwe L. Degree of hydration-based description of mechanical properties of early age concrete. Mater Struct 1996;29:335–44.
[20] Craeye B, De Schutter G. Experimental evaluation of mitigation of autogenous shrinkage by means of a vertical dilatometer for concrete. In: Jensen OM, Lura P, Kovler K, editors. International RILEM conference on volume changes of hardening concrete: testing and mitigation, 20–23 August, Lyngby, Denmark; 1996. p. 21–30.
[21] Staquet S, Boulay C, D'Aloia L, Toutlemonde F. Autogenous shrinkage of a self-compacting VHPC in isothermal and realistic temperature conditions. In: Marchand J, Bissonnette B, Gagné R, Jolin M, Paradis F, editors. 2nd International RILEM symposium on advances in concrete through science and engineering, 11–13 September, Quebec City, Canada; 2006. 15p.
[22] Jensen OM, Hansen PF. Influence of temperature on autogenous deformation and relative humidity change in hardening cement paste. Cem Concr Res 1999;29:567–75.
[23] Bjøntegaard Ø, Sellevold EJ. Interaction between thermal dilation and autogenous deformation in high performance concrete. Mater Struct 2001;34:266–72.
[24] Heldund H, Jonasson J-E. Temperature effect on autogenous deformation: measurements and modelling of thermal and moisture related deformation and stresses, IPACS report; 2001. 27p.
[25] Turcry P, Loukili A, Barcelo L, Casabonne JM. Can the maturity concept be used to separate the autogenous shrinkage and thermal deformation of a cement paste at early age? Cem Concr Res 2002;32:1443–50.
[26] Kamen A, Dénarié E, Sadouki H, Brühwiler E. Thermo-mechanical response of UHPFRC at early age – experimental study and numerical simulation. Cem Concr Res 2008;38:822–31.
[27] Bjøntegaard Ø. Thermal dilation and autogenous deformation as driving forces to self-induced stresses in high performance concrete. PhD thesis, NTNU, Norway; 1999. 256p.
[28] Mehta PK, Monteiro PJM. Concrete: microstructure, properties and materials. USA: McGraw-Hill; 2006. 659p.
[29] Diamond S. Mercury porosimetry – an inappropriate method for the measurement of pore size distributions in cement-based materials. Cem Concr Res 2000;30:1517–25.
[30] Kourounis S, Tsivilis S, Tsakiridis PE, Papadimitriou GD, Tsibouki Z. Properties and hydration of blended cements with steelmaking slag. Cem Concr Res 2007;37:815–22.
[31] Pal SC, Mukherjec A, Pathak SR. Investigation of hydraulic activity of ground granulated blast furnace slag in concrete. Cem Concr Res 2003;33:1481–6.
[32] Sant G, Rajabipour F, Lura P, Weiss J. Examining time-zero and early age expansion in pastes containing shrinkage reducing admixtures (SRA'S). In: Marchand J, Bissonnette B, Gagné R, Jolin M, Paradis F, editors. 2nd international RILEM symposium on advances in concrete through science and engineering, 11–13 September, Quebec City, Canada; 2006. 11p.
[33] Igarashi S, Watanabe A. Experimental study on prevention of autogenous deformation by internal curing using super-absorbent polymer particles. In: Jensen OM, Lura P, Kovler K, editors. Volume changes of hardening concrete: testing and mitigation, international RILEM conference, 20–23 August, Lyngby, Denmark; 2006. p. 77–86.
[34] Cusson D. Effect of blended cements on efficiency of internal curing of HPC, ACI SP-256. In: Internal curing of high-performance concrete: laboratory and field experiences. Farmington Hills, MI; 2008. p. 105–20.
[35] Eppers S, Mueller C. Autogenous shrinkage and time-zero of UHPC determined with the shrinkage cone, creep, shrinkage and durability of concrete and concrete structures. In: Tanabe T, Sakata K, Mihashi H, Sato R, Maekawa K, Nakamura H, editors. Proceedings of the 8th international conference, 30 September-2 October, Ise-Shima, Japan; 2008. p. 709–14.
[36] Hammer TA, Bjøntegaard Ø. Testing of autogenous deformation and thermal dilation of early age mortar and concrete – recommended test procedure. In: Jensen OM, Lura P, Kovler K, editors. International RILEM conference on volume changes of hardening concrete: testing and mitigation, 20–23 August, Lyngby, Denmark; 2006. p. 341–6.
[37] Atrushi DS. Tensile and compressive creep of early age concrete: testing and modelling, PhD thesis, Trondheim, Norway; 2003. 314p.
[38] Lura P. Autogenous deformation and internal curing of concrete, DTU, The Netherlands, PhD thesis; 2003. 180p.
[39] Bentz DP, Stutzman PE. Evolution of porosity and calcium hydroxide in laboratory concretes containing silica fume. Cem Concr Res 1994;24:1044–50.
[40] Baroghel-Bouny V, Mounanga P, Khelidj A, Loukili A, Rafaï N. Autogeneous deformations of cement pastes – Part II. W/C effects, micro–macro correlations and threshold values. Cem Concr Res 2006;36:123–36.